Materials Science and Engineering, 54 (1982) 113 - 120

Correlation Between Texture and Substructure of Conventionally and Shock-wave-deformed Aluminum

ASHOK G. DHERE*

Department of Metallurgical Engineering and Materials Science, University of Kentucky, Lexington, KY (U.S.A.)

HANS-JURGEN KESTENBACH*

Federal University of Sao Carlos, Sao Carlos, Sao Paulo (Brazil)

MARC A. MEYERS*

Department of Metallurgical and Materials Engineering, New Mexico Institute of Mining and Technology, Socorro, NM (U.S.A.)

(Received May 26, 1981; in revised form October 13, 1981)

SUMMARY

The changes in texture and substructure induced in commercial purity aluminum by conventional (cross-rolling) and shock wave deformation (peak pressure, 5.8 GPa; pulse duration, 2.8 μs) were studied by X-ray diffraction and transmission electron microscopy. Three different grain sizes were investigated (26, 70 and 440 μm) and shock wave deformation did not produce any noticeable change in texture, while cold rolling induced significant changes. The deformation substructure consisted of tangled dislocations after shock loading and of cellular arrays after rolling. Misorientations within the grains were investigated using Kikuchi lines and were found to be small after both shock loading and rolling (to an equivalent hardness).

1. INTRODUCTION

Shock wave deformation of metals is in many ways a unique deformation process. Strain rates of the order of 10^6 s^{-1} or higher are generated by the passage of a shock wave throughout the metal. The deformation substructures and residual mechanical properties can differ substantially from those of conventionally deformed metals. A great number of investigations have been devoted to shock loading over the past 30 years [1]. An unresolved problem, texture changes induced by the passage of the shock wave, was addressed in the investigation whose results are described herein. De Angelis and Cohen [2] observed texture changes in shock-loaded copper, while Higgins [3] and Trueb [4] report no such changes for copper and nickel respectively. De Angelis and Cohen [2], using inverse pole figures, suggested that the shock loading of copper (at peak pressures between 7.5 and 43.5 GPa) produced rotation of the grains, with an associated change in texture. The interpretation of their results was complicated by the presence of deformation twins; however, they were able to separate this effect from the general rotation of the grains. Monocrystalline copper, in contrast, did exhibit rotation of the order of 0.2° or less. Higgins [3] found results that conflicted with those of De Angelis and Cohen [2]; polycrystalline copper shocked at a pressure of approximately 43 GPa did not exhibit any appreciable change in texture. The misorientation within one single grain was found to be of the order of 4°. This value is too small to change the texture. Trueb [4] shock loaded nickel; internal misorientations of 1° or less were observed, with no change in texture.

Changes in texture can be caused by any of the three following mechanisms: (a) the grains can undergo a full rotation; (b) they can bend so that the orientation on one side is different from the other; (c) they can

*All previously at Center for Materials Research, Instituto Militar de Engenharia, Rio de Janeiro, RJ, Brazil.

0025-5416/82/0000-0000/$02.75

undergo a substructural rearrangement such as polygonization, with different regions forming different orientations. Any of these three mechanisms is theoretically possible in shock loading. The investigative effort described here addressed this problem using two techniques: X-ray diffraction to detect texture changes and transmission electron microscopy to establish the residual substructure and misorientations within the individual grains.

Commercially pure aluminum was chosen because (a) no twinning or any complicating transformation is induced in it by shock loading and (b) the texture effects had not been studied previously for this metal. Shock-loaded aluminum has been investigated previously by Rose and Berger [5], Appleton and Waddington [6], Otto and Mikesell [7], Krichenko and Rozhansky [8] and Parameswaran [9]. To the present authors' knowledge, the first report on the dislocation substructure is that by Rose and Berger [5]. They described the defect configuration as consisting of random heavily jogged dislocations on which a high density of dislocation loops and point defect clusters were superimposed.

2. EXPERIMENTAL TECHNIQUES

2.1. Materials and treatments

Three groups of samples with different grain sizes were prepared by successive reductions (by cold rolling in a Fenn rolling mill) and annealing treatments of commercially pure aluminum (99.5 wt.% Al; 0.01 wt.% Cu; 0.03 wt.% Fe; 0.03 wt.% Mg; 0.3 wt.% Si; 0.1 wt.% Zr) plate, with an initial thickness of 12.7 mm. Since grain growth in aluminum is greatly dependent on the amount of prestraining, different amounts of reductions were applied on the last reduction pass in order to produce different grain sizes; the smaller the amount of reduction, the greater is the resultant grain size [10]. A reduction of 76% followed by an anneal (for 1 h) at 380 °C yielded an average grain size of 26 μm; a reduction of 60% followed by an anneal (for 1 h) at 500 °C yielded a 70 μm grain size; a reduction of 10% followed by an anneal (for 1 h) at 500 °C yielded a 440 μm grain size. Optical microscopy was conducted after the specimens had been electropolished and etched using Barker's reagent (2% HBF in distilled water).

2.2. Shock wave deformation

Shock loading was conducted in a standard mousetrap-type system which is shown in Fig. 1. The system was propelled into a water pond that was dug in sand; the sand and water acted as cooling and decelerating media. The shock wave parameters and system dimensions were calculated using the procedures outlined by De Carli and Meyers [11]; a copper flyer plate (6.35 mm thick), accelerated from an initial stand-off distance of 9 mm by means of the explosive Plastex-P (the Brazilian equivalent of Detasheet C), provided a pressure pulse with the following initial parameters: peak pressure, 5.8 GPa; pulse duration, 2.8×10^{-6} s. Each grain size was separately shock loaded, and the protective cover plate had the same grain size as the plate used in subsequent experiments.

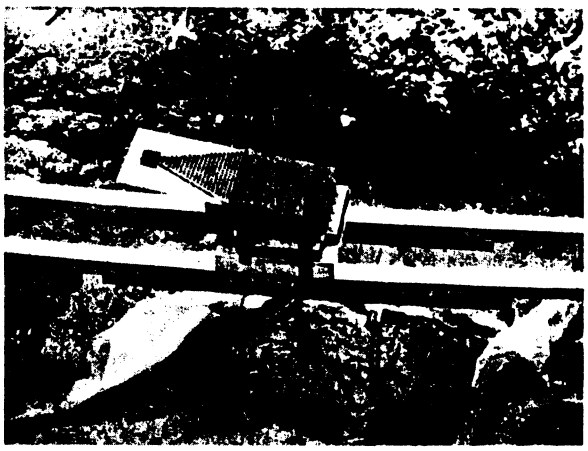

Fig. 1. System used for the generation of planar normal shock waves.

2.3. Cross-rolling

Cross-rolling was chosen to compare the effects of shock wave and conventional deformation because it provides a stress state somewhat similar to the uniaxial strain state of shock wave deformation. The sheets were rolled on a Fenn rolling mill by rotating them 90° prior to each pass. The reduction used for comparison purposes was the one providing the same hardness as that of the shock-loaded specimens. It has been shown that the

reduction to either an equivalent effective strain [12] or an equivalent shear strain [13] does not produce mechanical properties equivalent to those induced by shock loading. The reduction that provided the same hardness was, for the three grain sizes, 18%. In order to verify whether the strain was reasonably uniform throughout the thickness of the sheets, microhardness measurements were made across the cross section for the 26 μm and 440 μm sheets; the difference between the hardness of the surface and that of the interior was not found to be significant. The specimens were stored at −10 °C after both shock loading and rolling to prevent any possible recovery; no recovery of commercially pure aluminum even after 10 000 h at ambient temperature is reported in the *Metals Handbook* [14].

2.4. Texture determination by X-ray diffraction

A Philips PW-1140 diffractometer operated at 90 kV and 20 mA with a molybdenum tube and a zirconium filter was used. The changes in texture induced by deformation were monitored by determining the changes in the intensity of the principal peaks. Only diffraction peaks occurring at Bragg angles of less than 43° were analyzed. The intensities were corrected for background radiation. The texture parameter of a general peak i is calculated from the equation used for the determination of inverse pole figures [15, 16]:

$$T_i = \frac{I_i^{\mathrm{T}}}{\Sigma I_i^{\mathrm{T}}} \Big/ \frac{I_i^{\mathrm{R}}}{\Sigma I_i^{\mathrm{R}}}$$

where the superscripts T and R refer to the textured and random specimens respectively. The intensities of the peaks for the textureless (random) specimen were calculated using the method described by Cullity [17]; structure, multiplicity, Lorentz–polarization and temperature factors were included in the calculation. The specimen mount in the diffractometer had an oscillating capability, which was used to increase the number of grains analyzed. The procedure developed to calculate the number of grains included in the analysis is described by Dhere [18]. The samples were chemically polished prior to X-ray diffraction in order to remove any residue of a work-hardened surface layer.

2.5. Transmission electron microscopy

The specimens were prepared parallel to the sheet surface by spark erosion cutting followed by electrolytic polishing in a solution of 20% perchloric acid in alcohol. A JEOL model JEM-100 transmission electron microscope operating at 100 kV was used. Bright field transmission electron microscopy was used to reveal the dislocation substructure; the changes in the position of the Kikuchi lines observed in diffraction were used to establish the changes in orientation within the individual grains. All Kikuchi patterns were obtained from circular areas of 0.37 μm diameter, as measured from the size of the focused selected area diffraction aperture on the photograph. Orientation differences were determined between adjacent subgrains or by scanning entire grains along 5 μm intervals. Particular attention was given to the question whether or not small orientation differences between two adjacent areas accumulated over larger distances.

Inaccurate focusing of the diffraction aperture (which can be minimized but not avoided) and spherical aberration of the objective lens can easily lead to a displacement of the selected area for diffracted beams by several tenths of a micrometer [19]. Thus, the Kikuchi poles used for the orientation measurements may have been generated by crystal regions adjacent to the area actually observed in the diffraction aperture. For Kikuchi poles lying far away from and on opposite sides of the optical axis of the microscope (see, for example, Fig. 5, points 3 and 4), the area displacement error may have amounted to about 0.5 μm. However, such an error should not seriously affect the determination of orientation differences between 2 μm subgrains or between crystal regions which are spaced 5 μm apart.

3. RESULTS AND DISCUSSION

3.1. X-ray diffraction

Tables 1 and 2 show the texture parameters for the annealed, shock-loaded and cross-rolled specimens with grain sizes of 26 μm and 70 μm respectively. The number of grains included in the determination of the texture parameters of the specimen with a 440 μm grain size was not sufficient to be statistically

TABLE 1

Texture factors for annealed (T_A), shocked (T_S) and rolled (T_{R18}, T_{R60}) specimens with a 26 μm grain size

Plane	T_A	T_S	T_{R18}	T_{R60}	T_S/T_A	T_{R18}/T_A	T_{R60}/T_A
(111)	0.07	0.08	0.22	0.07	1.11	3.21	0.99
(200)	4.13	3.99	3.29	1.86	0.97	0.80	0.45
(220)	0.11	0.12	0.57	2.39	1.02	5.04	20.99
(311)	0.63	0.79	0.82	1.33	1.26	1.31	2.13
(331)	0.11	0.10	0.33	0.28	0.97	3.11	2.59
(420)	0.27	0.32	0.54	2.03	1.16	1.98	7.46
(422)	0.11	0.12	0.26	0.30	1.17	2.47	2.83
(620)	0.32	0.25	0.57	0.00	0.78	1.78	0.00
(642)	0.16	0.23	0.48	0.00	1.46	3.01	0.00

TABLE 2

Texture factors for annealed (T_A), shocked (T_S) and rolled (T_R) specimens with a 70 μm grain size

Plane	T_A	T_S	T_{R18}	T_S/T_A	T_{R18}/T_A
(111)	0.63	0.43	0.62	0.69	0.98
(200)	2.27	2.79	2.53	1.23	1.12
(220)	0.47	0.46	0.35	0.97	0.74
(311)	0.82	0.72	0.73	0.88	0.89
(331)	0.77	0.76	0.60	0.99	0.78
(420)	0.89	0.90	0.69	1.02	0.79
(422)	1.16	0.92	0.87	0.79	0.75
(620)	0.67	0.62	0.67	0.93	1.01
(642)	1.66	0.35	0.86	0.21	0.52

significant. For this reason the results are not included here.

The calculated numbers of grains [18] analyzed by the diffractometer during the scan for the three grain sizes are shown in Table 3. For the 26 μm, 70 μm and 440 μm grain sizes they are approximately equal to 10^5, 10^4 and 10^3 respectively. It can be seen that these numbers increase with increasing θ. Of these grains, only a very small fraction are actually oriented parallel to the surface at specific orientations. The calculated numbers of grains oriented for diffraction in several directions are given in parentheses in Table 3. It can be seen that, for example, 55.11 grains (111) are diffracted for the specimen with a 26 μm grain size, while only 1.31 grains of the same orientation are diffracting for the specimen with a 440 μm grain size. This shows quite clearly that the number of grains is not sufficient for the latter case. The texture parameters for the annealed, shocked and

TABLE 3

Number of grains analyzed by X-ray diffraction in each position for the three grain sizes

Orientation	*Number of grains analyzed for the following grain sizes*		
	26 μm	*70 μm*	*440 μm*
(111)	1.88×10^5 (55.1)	4.55×10^4 (22.3)	1.67×10^3 (1.31)
(200)	1.88×10^5 (41.2)	4.55×10^4 (16.7)	1.67×10^3 (1.0)
(220)	1.57×10^5 (67.7)	3.80×10^4 (27.3)	1.39×10^3 (1.6)
(311)	1.34×10^5 (113.9)	3.25×10^4 (46.0)	1.19×10^3 (2.7)
(331)	1.02×10^5 (91.0)	2.47×10^4 (36.7)	9.02×10^2 (2.1)
(420)	9.91×10^4 (40.6)	2.41×10^4 (16.5)	8.79×10^2 (1.0)
(422)	9.08×10^4 (73.1)	2.20×10^4 (29.5)	8.03×10^2 (1.7)
(620)	7.02×10^4 (26.0)	1.70×10^4 (8.9)	6.22×10^2 (0.62)
(642)	5.94×10^4 (40.0)	1.44×10^4 (17.3)	5.26×10^2 (0.9)

The numbers in parentheses represent the number of grains with their surface in the respective orientation, on the assumption of a random orientation (no texture).

rolled conditions are designated T_A, T_S and T_R respectively. A texture parameter of zero means that the respective peak is effectively non-existent; a texture parameter of unity indicates complete randomness with respect to that orientation. As can be seen, the texture parameters are different for the two grain sizes in the annealed condition. The system with a 26 μm grain size underwent a greater rolling reduction prior to annealing and shows

a more marked (100) texture; the texture parameters for (200) are equal to 4.1, 2.3 and 2.0 for specimens with grain sizes 26 μm, 70 μm and 440 μm respectively. The (100) texture is called cube texture [20].

It is customary to analyze only the principal peaks in inverse pole figures. Therefore, attention should be focused on the (100), (110), (111) and (311) peaks. For the lower intensity peaks the scatter and error are greater.

The main conclusion to be drawn from Tables 1 - 3 is that shock loading does not produce any appreciable change in the texture parameters. This result agrees with the conclusions of Trueb [4] and Higgins [3].

The ratio of the texture parameter in the shocked condition to that in the annealed condition, T_S/T_A, does not deviate substantially from the ratio for the principal planes. For the cross-rolled specimen, in contrast, changes in texture can be clearly seen. This can be most clearly seen for the 60% reduction specimen (T_{R60}). The ratio T_{R60}/T_S is equal to about 21 for the (110) plane. Hence, a strong rotation of the grains towards (110) can be seen. At 18% reduction the ratio T_{R18}/T_A is equal to 5. For the 70 μm specimen this effect is not observed; no drastic change in texture takes place. It seems that the initial texture is less amenable to changes in subsequent deformation.

3.2. Transmission electron microscopy

Typical dislocation substructures of the shock-loaded specimens are shown in Fig. 2. A uniform distribution of dislocations can be seen; no cells can be distinguished. The grain size does not seem to have a significant effect on the dislocation density. The dislocation substructure is similar to that observed by Rose and Berger [5]. The uniform dislocation distribution shows that no recovery has taken place. It is in accord with a model for dislocation generation proposed by Meyers [21, 22]. This model suggests that dislocations are homogeneously nucleated at the shock front by the powerful deviatoric shear stresses (about 3 GPa) set up by the shock wave. These dislocations cannot advance with the front and are left behind. No conventional generation mechanisms, such as Frank–Read sources, are required to operate. It is believed that, in aluminum, little dislocation reorganization takes place after the passage of the front; in nickel and copper, both

(a)

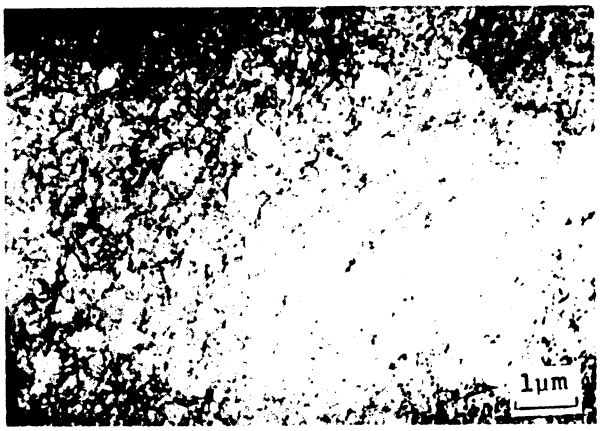

(b)

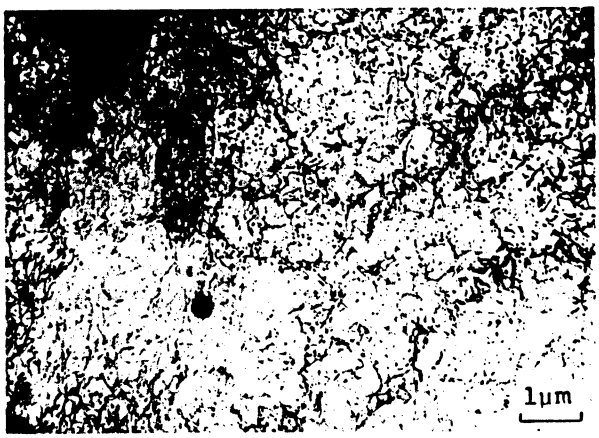

(c)

Fig. 2. Deformation substructure after shock loading at a 5.8 GPa peak pressure and a 2.8 μs pulse duration for three grain sizes: (a) 26 μm; (b) 70 μm; (c) 440 μm.

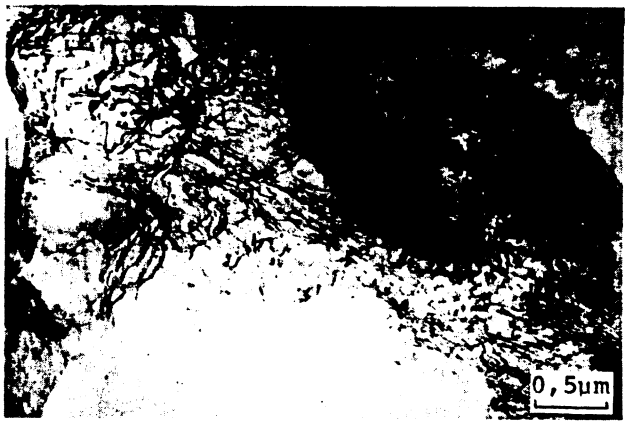

(a)

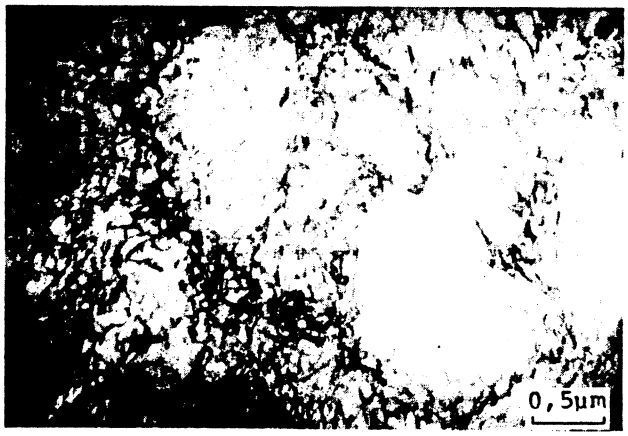

(b)

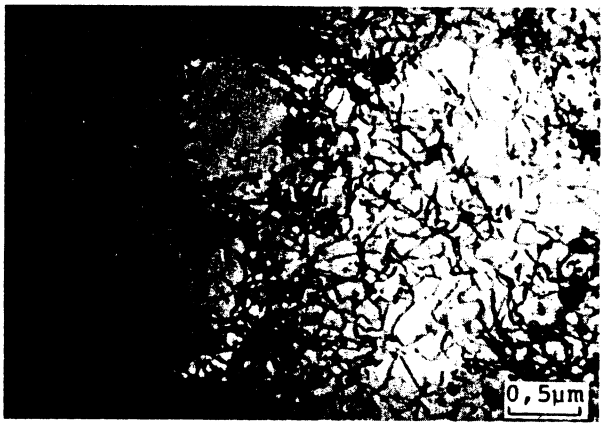

(c)

Fig. 3. Deformation substructure after cross rolling to a reduction of 18% for three grain sizes: (a) 26 μm; (b) 70 μm; (c) 440 μm.

medium or high stacking fault energy f.c.c. metals, the dislocations tend to arrange themselves into cells after shock loading.

Another feature that deserves comment is the clustering of point defects. The small dark spots in Fig. 2 are due to vacancy or interstitial clusters; Rose and Berger [5] identified these clusters and quantitatively established their density as 1.9×10^{15} cm^{-3} for a specimen shock loaded to a peak pressure of 6.5 GPa. Figure 2 suggests that the number of these clusters is higher in the specimen with a large grain size. Any explanation on the matter is speculatory, but it could be hypothesized that there are fewer grain boundaries (excellent point defect sinks) for the specimen with a large grain size, and the point defects have a stronger tendency to cluster. Shock-loaded copper and nickel, however, do not exhibit these clusters. This is probably due to the lower mobility of point defects at ambient temperature for these higher melting point metals.

The substructure of the cross-rolled specimens (cross rolled to the same hardness as the shocked specimens, 18% reduction) are shown in Fig. 3. Dislocations are arranged in cells; the cell size is approximately equal to 2 μm. If the reduction by cold rolling is increased, the cell walls become better and better defined until they form a subboundary. Figure 4 shows the subgrains after 60% reduction, for the specimen with a 26 μm grain size. Subgrain formation occurs when the misorientation between adjacent cells reaches a critical value. The point defect clusters are much less numerous after rolling than shocking, confirming the experimental measurements of Kressel and Brown [23].

Fig. 4. Deformation substructure after cross rolling to a reduction of 60% (specimen with a 26 μm grain size).

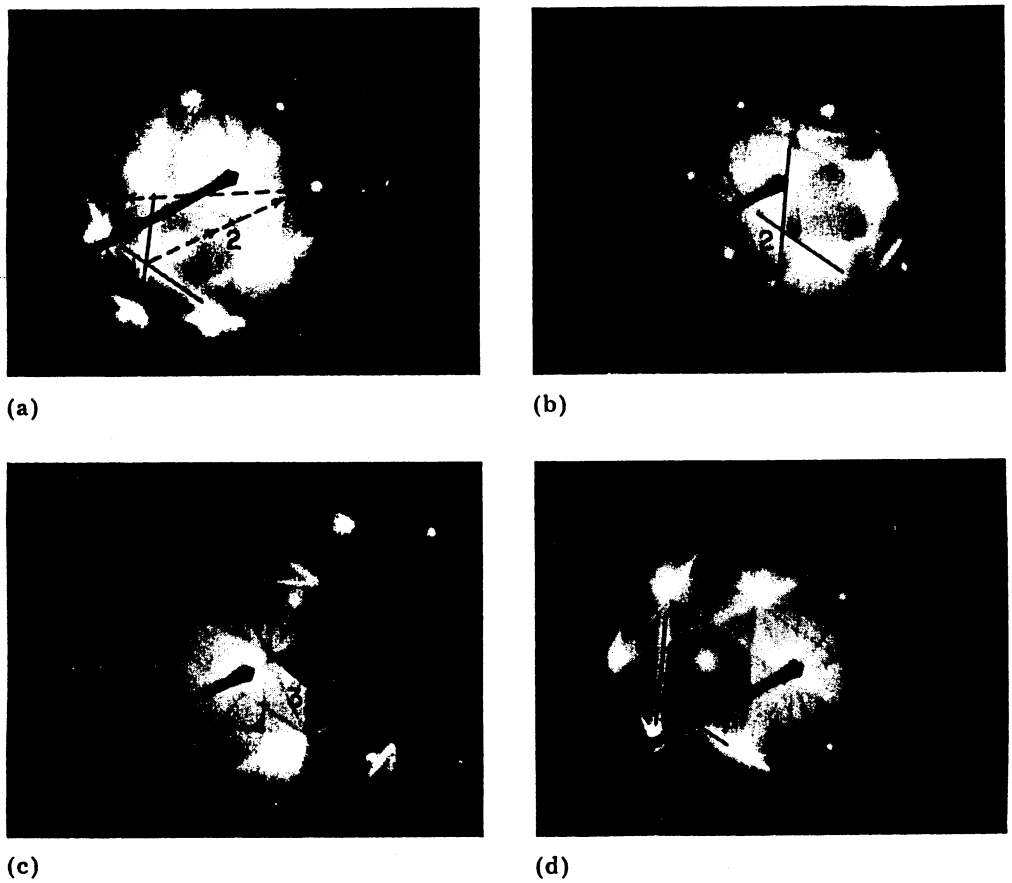

Fig. 5. Movement of Kikuchi diffraction lines (specimen with a 26 μm grain size cross rolled to 18% reduction) with the change in orientation within the grain; the four points 1, 2, 3, 4 are represented separately in (a) - (d) and simultaneously in (a).

Murr *et al.* [24] and Graham [25] also found high point defect densities after shock loading.

The changes in orientation within the individual grains were measured by the Kikuchi line technique. Figure 5 illustrates this technique for the rolled specimen (grain size, 26 μm). Points 1, 2, 3 and 4 show the positions of a given Kikuchi pole which correspond to the orientations of four different crystal regions within one grain. These different points are simultaneously represented in Fig. 5(a); the misorientation is calculated, knowing that these points are on the surface of a sphere with a radius L of 54.55 cm. The angle between points 1 and 2 is 1.57°, that between points 2 and 3 is 1.21° and that between points 3 and 4 is 3.36°. These observations were made by moving the specimen by approximately 5 μm between consecutive points along a fixed direction within the grain. For the 70 μm cross-rolled specimen, the misorientations found were similar: 1° between adjacent cells, 2° over a distance of 5 μm and 3.5° - 4° over greater distances within one grain. The specimen with a 440 μm grain size (cross rolled) showed misorientations of about 1° over a distance of 15 μm and of 3.5° if the position of the beam was displaced by 120 μm. The specimen cold rolled to a 60% reduction exhibited greater misorientation within the grains due to the formation of subgrains; this agrees with the proposal of Barrett and Levenson [26]. Abrupt changes in orientation in adjacent areas of a same grain were observed; the angle was not measured.

The shocked specimens with 26 and 70 μm grain sizes exhibited maximum misorientations of 2° over the whole extent of the grain. Misorientations of 1° were observed over distances of 5 μm; nevertheless, they did not add up over larger distances. These misorienta-

tions are lower than those for specimens with the same grain size cross rolled 18%. For the specimen with a 440 μm grain size, the misorientation over distances of the order of 15 μm was approximately 1.5°. Over a distance of 60 μm, the misorientation was 4.3°.

4. CONCLUSIONS

(a) Shock wave deformation of commercial purity aluminum to a peak pressure of 5.8 GPa and a pulse duration of 2.8 μs does not lead to any substantial change in the texture. Continuous changes in orientations within the grains are small, and no grain fragmentation was observed.

(b) The cross-rolling of similar specimens to reductions in thickness of 18% and 60% leads to the following.

(i) The changes in texture are small at 18% reduction; they are dependent on the initial texture of the specimen. After 60% reduction, a strong (110) texture is produced for the specimen with a 26 μm grain size.

(ii) Continuous changes in orientation are observed within the grain; at 18% reduction they do not seem to add up over large extensions. For the 60% reduction, the misorientation is large, consistent with the fact that the substructure shows subgrain formation.

(c) Continuous changes of orientation within one grain seem to be limited to a maximum of 5°. Beyond this value the grain fragments into subgrains separated by small-angle boundaries.

ACKNOWLEDGMENTS

Professor A. Saavedra, Instituto Militar de Engenharia, and Professor R. J. De Angelis, University of Kentucky, were very helpful in the interpretation of the X-ray diffraction data; Professor F. D. S. Marques, South Dakota, provided invaluable help in the later stages of this investigation. The help of the Marambaia Proving Ground personnel on the execution of the explosive events is gratefully acknowledged. The explosive Plastex-P was developed by Cap. Rocha of the Piquete Explosives Plant.

This research was supported by Financiadora de Estudos e Projetos through the Materials Research Center, Instituto Militar de Engenharia. The National Science Foundation grant DMR 79-27102 is gratefully acknowledged by one of us (M.A.M.).

REFERENCES

1 M. A. Meyers and L. E. Murr (eds.), *Shock Waves and High-strain-rate Phenomena in Metals: Concepts and Applications*, Plenum, New York, 1981.
2 R. J. De Angelis and J. B. Cohen, *Trans. Am. Soc. Met., 58* (1965) 700.
3 G. T. Higgins, *Metall. Trans., 2* (1971) 1277.
4 L. F. Trueb, *J. Appl. Phys., 40* (1967) 2976.
5 M. F. Rose and T. L. Berger, *Philos. Mag., 17* (1968) 1121.
6 A. S. Appleton and J. S. Waddington, *Philos. Mag., 12* (1965) 273.
7 H. E. Otto and R. Mikesell, *Proc. 1st Int. Conf. on High Energy Rate Formation, University of Denver, 1967.*
8 V. V. Krichenko and V. N. Rozhansky, *Phys. Met. Metallogr. (U.S.S.R.), 36* (1974) 177.
9 V. R. Parameswaran, *Scr. Metall., 9* (1975) 31.
10 W. A. Anderson, *Aluminum*, Vol. I, American Society for Metals, Metals Park, OH, 1967.
11 P. S. De Carli and M. A. Meyers, in M. A. Meyers and L. E. Murr (eds.), *Shock Waves and High-strain-rate Phenomena in Metals: Concepts and Applications*, Plenum, New York, 1981, p. 341.
12 M. A. Meyers and R. N. Orava, *Metall. Trans. A, 7* (1976) 179.
13 H.-J. Kestenbach and M. A. Meyers, *Metall. Trans. A, 7* (1976) 1943.
14 *Metals Handbook*, Vol. I, American Society for Metals, Metals Park, OH, 1975, p. 936.
15 C. S. Barrett and T. B. Massalski, *The Structure of Metals*, McGraw-Hill, New York, 3rd edn., 1966.
16 J. R. C. Guimarães, A. Saavedra, R. M. Brito and J. C. Gomes, *Metallography, 9* (1976) 1.
17 B. D. Cullity, *Elements of X-ray Diffraction*, Addison-Wesley, Reading, MA, 1968.
18 A. G. Dhere, *M.Sc. Thesis*, Instituto Militar de Engenharia, Rio de Janeiro, Brazil, 1978.
19 P. B. Hirsch, A. Howie, R. B. Nicholson, D. W. Pashley and M. J. Whelan, *Electron Microscopy of Thin Crystals*, Butterworths, London, 1965, p. 18.
20 L. Frommer, *J. Inst. Met., 66* (1940) 264.
21 M. A. Meyers, *Scr. Metall., 12* (1978) 21.
22 M. A. Meyers, in P. Haasen, V. Gerold and G. Kostorz (eds.), *Proc. 5th Int. Conf. on the Strength of Metals and Alloys, Aachen, August 1979*, Pergamon, Oxford, 1980, p. 547.
23 H. Kressel and N. Brown, *J. Appl. Phys., 38* (1967) 1618.
24 L. E. Murr, O. T. Inal and A. A. Morales, *Acta Metall., 24* (1976) 261.
25 R. A. Graham, in M. A. Meyers and L. E. Murr (eds.), *Shock Waves and High-strain-rate Phenomena in Metals: Concepts and Applications*, Plenum, New York, 1981, p. 375.
26 C. S. Barrett and L. H. Levenson, *Trans. AIME, 137* (1940) 112.